

HOW TO REACH MORE PRECISE INTERPRETATION OF SUBGAP ABSORPTION SPECTRA IN TERMS OF DEEP DEFECT DENSITY IN a-Si:H

N. WYRSCH, F. FINGER

IMT, Neuchâtel University, Rue Breguet 2, CH-2000 Neuchâtel, Switzerland

T. J. McMAHON

Solar Energy Research Institute, Golden, CO 80401-3393, USA

M. VANECEK

Institute of Physics CSAV, Cukrovarnicka 10, 16200 Prague 6, Czechoslovakia

Values for the deep defect density determined from PDS, CPM or ESR may vary significantly on the same sample depending on the method of data analysis used. Experimental conditions under which they yield comparable results are discussed. Procedures for determination of deep defect density from optical spectra are reviewed and compared on samples in light-saturated states. The measurement of the absorption coefficient at $E=1.2$ eV, with a new range for the calibration factor, is suggested as an easy and generally usable procedure for the determination of deep defect density.

1. INTRODUCTION

To optimize amorphous silicon from the point of view of the highest long-term solar cell efficiency, it has now become important to optimize the deposition of the intrinsic layer by minimizing the deep defect density in the light-saturated state (and not in the "as grown" state). To do this, we have to measure precisely the number of spins N_s by Electron Spin Resonance (ESR) or the number of deep defect N_{dd} by Photothermal Deflection Spectroscopy (PDS) or Constant Photocurrent Measurement (CPM) in a well defined, light-soaked state. Optical measurements are often more convenient and available in most laboratories.

Even if optical measurements done in different laboratories give quite similar results, N_{dd} values deduced from such measurements differ appreciably. There exist at present 12 different procedures¹⁻¹² for interpreting the absorption data and they yield results spread over nearly one order of magnitude. Here, we will analyse the precision of PDS, CPM and ESR measurements and present different deconvolution procedures based on the assumption of the constancy of the optical transition matrix element with energy. Data on the calibration of defect absorption by ESR measurements on light-saturated samples will be given and compared to our method for the determination of deep defect density from optical absorption measurements in a-Si:H.

2. EXPERIMENTAL METHODS

PDS is a subgap absorption technique which measures *all* possible transitions from occupied to unoccupied states (cf Fig.1); surface, interface and substrate contributions are also included. Typically for a 1-2 μm thick a-Si:H sample in annealed (or as grown) state surface/interface absorption

dominates. Thus, it is difficult to get αd (absorption coefficient \times thickness) values below 1×10^{-4} . This technique has the advantages of giving *absolute* absorption values and to be only weakly dependent on the charge state of the deep defects.

CPM measures only transitions contributing to the photo-current, i.e. transitions leading to the excitation of carriers into extended states (cf Fig.1) in the high lifetime part of the sample. This technique is not sensitive to surface states if samples with thicknesses $d > 1.5 \mu\text{m}$ are used. Thus, sensitivities well below $\alpha d \approx 1 \times 10^{-5}$ can be achieved. CPM is a *relative* method which needs to be calibrated by means of another technique like optical transmission or PDS. As it measures only transitions contributing to the current, mostly occupied states are seen in the subgap absorption spectra (for intrinsic a-Si:H). This implies that this technique is Fermi level dependant.

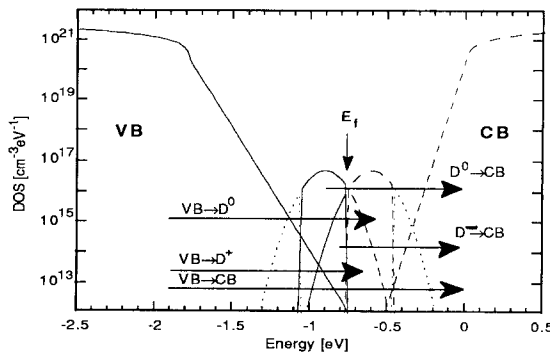


FIGURE 1
Possible optical transitions in a-Si:H. Transitions from VB to D^0/D^+ are almost not seen in CPM due to the low contribution of holes to the photo-current.

ESR measures *all* defects in the *paramagnetic* state (spins); it measures only D⁰ deep defects and does not see D⁺ and D⁻. It may also be influenced by surface, interface and substrate defects. Absolute numbers for the spin density are often difficult to obtain due to the differences in the fill factor of the cavity for the sample and for the spin standard, respectively (the response of the loaded cavity depends on the sample and substrate dimensions and their dielectric behaviour). Moreover, for a 1 cm² 2 μm thick sample, spin densities below 1x10¹⁶ cm⁻³ are usually completely masked by surface contributions. Also, additional contributions may be due to the substrate (like the E' centre in SiO₂) as well as due to background signals from carbon or metal impurities.

3. INTERPRETATION OF SUBGAP ABSORPTION SPECTRA

To interpret data from either PDS or CPM in terms of deep defect density, we have three basically different approaches. We can use

- 1) a deconvolution of the optical spectra^{2,3,11,12}
- 2) the "integrated excess absorption"^{1,4}
- 3) the absorption coefficient at a single energy^{5,6,8,10}

All of these different procedures need some calibration (usually by ESR) and/or assumptions as discussed below.

3.1 DECONVOLUTIONS

Deconvolution procedures, based on the formula linking the absorption coefficient $\alpha(E)$ as a function of energy to the density of occupied N_{initial} and unoccupied N_{final} states

$$\alpha(E) = \frac{\text{const}}{E} P^2(E) \int_{E_f}^E N_{\text{initial}}(\varepsilon) N_{\text{final}}(\varepsilon+E) d\varepsilon, \quad (1)$$

were applied to CPM spectra by a) the Prague group², b) the Marburg group¹¹, and c) by the Villeurbanne group¹² and to CPM and PDS spectra by d) the Neuchâtel group³.

It is usually assumed that the momentum matrix elements for the optical transitions $P^2(E)$ are constant¹³. The spectral dependence of the index of refraction ($n=3.6-4.4$ in the range 0.8-2 eV) is also neglected. Furthermore, some knowledge of the density of state (DOS) is needed. If details of the DOS in the gap region need not to be known for procedures b) and c) (the latter is a refinement of the former), they rely on a strong decrease in the DOS in the band-tails, on the free electron density value $n=6.7 \times 10^{21}$ cm⁻³ and on a fixed slope for the parabolic bands at the band edges. Procedure a) requires, in addition to the assumptions of parabolic bands and free electron density value, a Gaussian distribution of deep defects and exponential band-tails; then position, width and height of this Gaussian

distribution are fitted to the experimental data. Procedure d) may be applied to both CPM and PDS. It includes all transitions from occupied states to unoccupied states (Fig. 1), including the transitions from valence band (VB) to conduction band (CB) which are not taken into account in procedure a). It assumes a Gaussian deep defect distribution with positive correlation energy. Fermi level position (or the occupation of the deep defects), parabolic shape of the band and gap energy may be fitted. Instead of the free electron density value, it assumes a density of states $N=1 \times 10^{21}$ cm⁻³eV⁻¹ at the band edge, defined as the limit between the exponential band-tails and the parabolic band. The defect density is given by the integration over the deep defects DOS.

3.2 "INTEGRATED EXCESS ABSORPTION"

The "integrated excess absorption" is defined as the integration of the contribution of deep defects to the absorption up to the Urbach energy (exponential part of the absorption spectra), and is used as a measure of the deep defect density N_{dd} ¹

$$N_{\text{dd}} = k \int \alpha_{\text{ex}}(E) dE, \quad (2)$$

where $\alpha_{\text{ex}}(E) = \alpha(E) - \alpha_{\text{Urbach}}(E)$.

It is assumed that the optical transitions can be described by a two level system with a single "average" oscillator energy¹⁴; using the sum rule formula relating the density oscillators to their absorption, this leads to $k=7.9 \times 10^{15}$ cm⁻²eV⁻¹ for PDS measurements. But the "excess absorption" as defined by Jackson and Amer¹ (Fig. 2) is just a part of the total defect absorption. Most of the deep defect absorption is masked by the higher tail-to-band and band-to-band absorption. The deep defect absorption spans, as the broadening of the average band level, over a few eV. Thus, it is surprising that Jackson and Amer achieved such a good correspondence between the N_{dd} value determined from eqn.(2) with $k=7.9 \times 10^{15}$ cm⁻²eV⁻¹ and N_{dd} values from ESR measurements. Furthermore, this method has been criticized by Li and Paul¹⁵ who saw no physical reason to apply molecular vibrations theory to electronic excitations. They argue that the sum rule, that assumes a single excitation at a well defined energy cannot be applied to the case of transitions to a broad distribution of extended states. Even if this theoretical background of this method is physically questionable, it is functionally not very different from the third type of method described below. It can be seen as a way of averaging the absorption value over some energy range spread from the lowest energy up to the Urbach edge. Note that for CPM measurements, the

Princeton group⁴ found $k=1.9 \times 10^{16}$ by comparison with ESR spin density.

3.3 ABSORPTION COEFFICIENT AT A SINGLE ENERGY

In the band region, the value of DOS divided by E is almost constant in contrast to the DOS in the defect region. Therefore, using eqn.(1), we may link the absorption at a reference point E_{ref} with the deep defect density in the following manner:

$$\alpha(E_{\text{ref}}) = C(E_{\text{ref}}) N_{\text{dd}}, \quad (3)$$

where $C(E_{\text{ref}})$ is a weakly energy dependent constant.

If most of the authors take E_{ref} around 1.2 eV, the Marburg group⁵ takes E_{ref} at the crossing point between the Urbach edge and the deep defect contributions to the absorption. It should be noted that the determination of this point is somewhat arbitrary and its position is dependent on the Fermi level position and on the energy dependence assumed for the matrix elements.

Wang et al. suggested recently⁶ to take the reference point E_{ref} at the maximum of the excess, defect related absorption $\alpha_{\text{ex}}(E)$. However, this choice of reference point will be influenced by the slope of the Urbach tail, even in the absence of any change in the deep defect or band distribution of states.

Nevertheless, deep defect determination from the absorption at a single energy offers, for a *proper choice* of the reference energy point, as will be discussed below, the needed simplicity together with a reasonable accuracy.

4. PROCEDURE FOR THE CALIBRATION OF THE DEFECT ABSORPTION SPECTRUM

Defect absorption spectra with electron transitions from initial defect states to the conduction band can be divided into 4 parts (of Fig.2). Part I of the absorption spectrum reflects the defect level broadening and thermal broadening of the absorption spectrum. To get the true value of the deep defect absorption in region III, we have to subtract absorption between VB tail and CB. Defect absorption in region IV is fully hidden in the much stronger absorption from VB tail and from VB to CB. Therefore, region II and $E_{\text{ref}}=1.2$ eV is best used for calibration of the defect absorption (CPM) spectrum. This approach was pioneered by the Harvard group⁸. Each point on the defect absorption curve can be used for calibration (e.g. by ESR)¹⁶ if this point is more than $(W+D)$ higher in energy than E_I , the position of the defect from the CB, where $2W$ is the halfwidth of the Gaussian distribution and D , the thermal broadening, is about 0.1 eV at room temperature¹⁷.

For PDS spectra, assuming a deep defect centre energy $E_I \approx 0.9$ eV and a correlation energy of ≈ 0.3 eV, implies that the absorption coefficient between 1.1 and 1.2 eV remains almost insensitive to the Fermi level position. It corresponds approximately to the middle energy point between transitions from CB to unoccupied defects and transitions from occupied defects to VB. These arguments support the choice of 1.2 eV as a reasonable reference point.

One crucial assumption is that both optical defect absorption and ESR signal come from the same defects. A good way to solve this problem is to *create new defects in the material by light soaking*. This approach has also several experimental advantages: The Fermi level is pinned in the middle of the defect distribution giving us more than one half of dangling bonds in paramagnetic state D^0 regardless of the precise value of the correlation energy U , if $U \geq W$. Thanks to the higher defect density, the ESR signal is well above the signal due to surface and background spins. Effects from the E_f position are also minimized in CPM measurement and all the experimental $\alpha(E)$ curves have very similar shapes. With the assumption $U \geq W$ (which remains to be demonstrated), at least 3/4 of dangling bonds are in the D^0 or D^+ state and can be detected by CPM. So the number of deep defects seen by both techniques should differ by less than 50% (experimental errors excepted).

We have applied the deep defect determination procedures described in §3 on our experimental optical spectra of light-saturated samples. We have deduced for each procedure the corresponding calibration factors at $\alpha(1.2$ eV). These factors are summarized in Table 1 with respect to $\alpha(1.2$ eV)=1 cm⁻¹ for CPM spectra and $\alpha(1.2$ eV)=2 cm⁻¹ for PDS. The factor of 2 reflects the symmetry in hole and

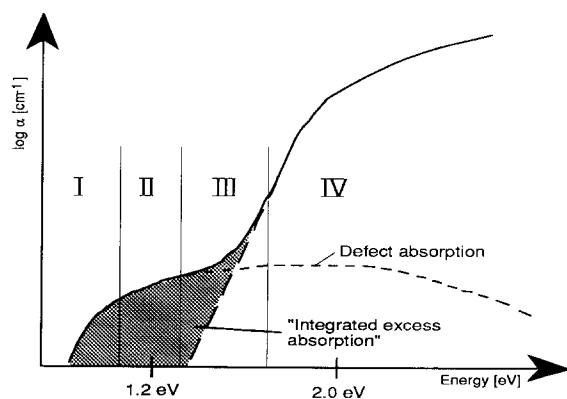


FIGURE 2
Schematic view of a CPM (or PDS) absorption spectra with the corresponding defect absorption contribution. Dashed area represents the integrated excess absorption.

electron transitions. Results fall into 3 groups: (1) for most of the data $\alpha(1.2 \text{ eV})=1 \text{ cm}^{-1}$ (measured by CPM) or $\alpha(1.2 \text{ eV})=2 \text{ cm}^{-1}$ (measured by PDS) corresponds to $1-2 \times 10^{16} \text{ cm}^{-3}$ dangling bonds. (2) The original estimate falls well below this range⁸. (3) On the other hand, our recent data, presented in Table II, are in the somewhat higher range

$$\alpha_{\text{CPM}}(1.2 \text{ eV})=1 \text{ cm}^{-1} \leftrightarrow 2.4-5 \times 10^{16} \text{ cm}^{-3}$$

We contend that the latter values, which were obtained on identical light saturated samples, should be more precise because of the above arguments.

5. CONCLUSIONS

We have discussed several approaches to determine the

$\alpha(1.2 \text{ eV})$	calibration method	$N_{\text{dd}} [\text{cm}^{-3}]$	Remark	Reference
1 cm^{-1} CPM	ESR	5×10^{16}	a)	10 SERI, Prague
1 cm^{-1} CPM	Deconvolution	2×10^{16}	a)	2 Prague
1 cm^{-1} CPM	ESR+LESR	1.5×10^{16}	b)	7 Kanazawa
1 cm^{-1} CPM	Full deconvolution	3×10^{16}	a),c)	3 Neuchâtel
1 cm^{-1} CPM	ESR	1.5×10^{16}	a)	5 Marburg
1 cm^{-1} CPM	Integrated absorption, ESR	1.3×10^{16}	a)	4,6 Princeton
1 cm^{-1} CPM	Capacitance measurement	1.5×10^{15} to 6×10^{15}	b),d)	8 Harvard
2 cm^{-1} PDS	Integrated absorption	1.2×10^{16}	c)	1 Xerox
2 cm^{-1} PDS	Full deconvolution	2.3×10^{16}	c)	3 Neuchâtel

TABLE I

Summary of relations between absorption at 1.2 eV and deep defect density N_{dd} using different calibration procedures given in references applied on a) a $2.3 \mu\text{m}$ thick light-saturated sample from GSI, on c) several light saturated $2-3 \mu\text{m}$ thick Neuchâtel samples. b) and d) were taken from the references. d) also assumes a "flat" DOS between the tails.

Sample	Thickness [μm]	$\alpha(1.2 \text{ eV})$ [cm^{-1}]	N_{dd} [cm^{-3}]	Method	calibration factor
GSI	2.3	1.67 CPM	8.2×10^{16}	ESR	5×10^{16}
"	"	1.67 CPM	5.4×10^{16}	deconv.	3×10^{16}
GSI	2.0	1.9 CPM	6.6×10^{16}	ESR	3.5×10^{16}
SERI	2.1	0.6 CPM	1.8×10^{16}	deconv.	3×10^{16}
Neuchâtel	3.2	7.2 CPM	1.8×10^{17}	ESR	2.4×10^{16}
"	"	12.3 PDS	"	"	2.9×10^{16}

TABLE II

$\alpha(1.2 \text{ eV})$ and deep defect density N_{dd} determined by ESR or full deconvolution on several light saturated samples and the corresponding calibration factor between $\alpha(1.2 \text{ eV})=1 \text{ cm}^{-1}$ for CPM ($=2 \text{ cm}^{-1}$ for PDS) and N_{dd} .

deep defect density in intrinsic a-Si:H. As an easy and sufficiently precise approach the value of the optical absorption at 1.2 eV can be used. Thereby, a higher precision of calibration is reached if samples in saturated light soaked state are investigated. Our experimental data suggest that if $\alpha(1.2 \text{ eV})$ as measured by CPM equals 1 cm^{-1} (or by PDS equals 2 cm^{-1}) the dangling bond density should be in the range $2.4-5 \times 10^{16} \text{ cm}^{-3}$. Precision of the method relies mostly on the precision of the calibration given by ESR, or alternative methods, and on the determination of the absolute absorption scale for CPM.

AKNOWLEDGMENTS

The authors would like to thank A. Shah for helpful discussions. This work was supported by the Swiss Federal Research Programme OFEN-REN under contract EF-REN 90(045) and by Czech grant no. 11053.

REFERENCES

1. W.B. Jackson, N.M. Amer, Phys. Rev. B25 (1982) 5559.
2. M. Vanecek, J. Kocka, J. Stuchlik, Z. Kozisek, O. Stika, A. Triska, Solar En. Mat. 8 (1983) 411.
3. M. Vanecek, A. Abraham, O. Stika, J. Stuchlik, J. Kocka, Phys. Stat. Sol. (a)83 (1984) 617.
4. H. Curtins, M. Favre in "Amorphous Silicon and Related Materials", ed. H. Fritzsche, World Scientific, Singapore, 1989, p. 329.
5. N. Wyrsch, Doctorate thesis, 1991.
6. C.R. Wronski, Z.E. Smith, S. Aljishi, V. Chu, K. Shepard, D.S. Shen, R. Schwarz, D. Slobodin, S. Wagner, AIP Conf. Proc. 157 (1987) 70.
7. K. Pierz, W. Fuhs, H. Mell, Phil. Mag. B63 (1991) 123.
8. N.W. Wang, X. Xu, S. Wagner, Int. Meeting on Stability of Amorphous Silicon Materials and Solar Cells, Denver, 1991, to be published.
9. T. Shimizu, H. Kidoh, A. Morimoto, M. Kumeda, Jap. Appl. Phys. 28 (1989) 586.
10. A. Lachter, R.L. Weissfield, W. Paul, Solar En. Mat. 7 (1982) 263.
11. K. Pierz, H. Mell, J. Terjukov, J. Non-Cryst. Sol. 77&78 (1985) 547.
12. P. Jensen, Sol. State. Comm. 76 (1990) 1301.
13. W.B. Jackson, C.C. Tsai, S.M. Kelso, J. Non-Cryst. Sol. 77&78 (1985) 281.
14. S.H. Wemple, J. Chem. Phys. 67 (1977) 2151.
15. Y.-M. Li, W. Paul, MRS Symp. Proc., Anaheim, 1991, to be published.
16. W. Schelter, W. Hell, R. Helbig, M. Schulz, J. Phys. C: Sol. State Phys. 15 (1982) 5839.
17. M. Jaros, Phys. Rev. B16 (1977) 3694.